Development 136, 2913-2921 (2009) doi:10.1242/dev.038935

Control of extracellular matrix assembly along tissue boundaries via Integrin and Eph/Ephrin signaling

Dörthe Jülich[1], A. Paul Mould[2], Ewa Koper[2] and Scott A. Holley[1,*]

Extracellular matrixes (ECMs) coat and subdivide animal tissues, but it is unclear how ECM formation is restricted to tissue surfaces and specific cell interfaces. During zebrafish somite morphogenesis, segmental assembly of an ECM composed of Fibronectin (FN) depends on the FN receptor Integrin α5β1. Using in vivo imaging and genetic mosaics, our studies suggest that incipient Itgα5 clustering along the nascent border precedes matrix formation and is independent of FN binding. Integrin clustering can be initiated by Eph/Ephrin signaling, with Ephrin reverse signaling being sufficient for clustering. Prior to activation, Itgα5 expressed on adjacent cells reciprocally and non-cell-autonomously inhibits spontaneous Integrin clustering and assembly of an ECM. Surface derepression of this inhibition provides a self-organizing mechanism for the formation and maintenance of ECM along the tissue surface. Within the tissue, interplay between Eph/Ephrin signaling, ligand-independent Integrin clustering and reciprocal Integrin inhibition restricts de novo ECM production to somite boundaries.

KEY WORDS: Eph, Ephrin, Fibronectin, Integrin, Morphogenesis, Zebrafish

INTRODUCTION

Integrins are heterodimeric transmembrane proteins composed of an α and a β subunit that link the actin cytoskeleton to the extracellular matrix (ECM) (Bokel and Brown, 2002; Ginsberg et al., 2005; Hynes, 2002). Integrins function as an allosteric switch that transduce signals bidirectionally across the plasma membrane and are important for cell migration, adhesion and cell survival. Transduction of signals from the extracellular space to the cytoplasm, called 'outside-in' signaling, can result in cytoskeletal rearrangement and changes in gene expression. Cytoplasmic signals can initiate 'inside-out' signaling by inducing a conformational change to a high-affinity ligand-binding state (Askari et al., 2009; Bokel and Brown, 2002; Ginsberg et al., 2005; Hynes, 2002; Shimaoka et al., 2002). Inside-out signaling can also cause Integrin clustering (Alon and Feigelson, 2002). Both affinity changes and clustering lead to increased avidity of Integrins for ECM macromolecules. Integrin α5β1 (Itgα5β1) is the primary receptor for Fibronectin (FN) and is required for FN matrix assembly. Matrix assembly is thought to proceed via Itgα5β1 binding to FN, clustering of the Integrin and cross-linking of FN. The cross-linking of FN depends upon the application of tension from the actin cytoskeleton through Itgα5β1, which stretches FN dimers thereby revealing FN binding sites within FN itself (Larsen et al., 2006; Mao and Schwarzbauer, 2005a). In vivo, tension within tissues mediated by Cadherin cell-cell adhesion promotes FN matrix assembly (Dzamba et al., 2009). However, most of our understanding of EMC assembly comes from studies in 2D cell culture, although subsequent analyses in 3D culture suggest the regulation and cellular responses to Itgα5β1 differ in these more complex environments (Cukierman et al., 2001; Larsen et al., 2006; Mao and Schwarzbauer, 2005a; Mao and Schwarzbauer, 2005b). Separate genetic analyses have broadly defined the roles of Integrins in vivo and specifically have indicated that *itga5* and *fn* are required for somite formation in mouse, zebrafish and *Xenopus* (Georges-Labouesse et al., 1996; Hynes, 2002; Jülich et al., 2005; Koshida et al., 2005; Kragtorp and Miller, 2007; Yang et al., 1999). Somites are the segmented anlagen of the skeletal muscle and vertebral column. During somite border morphogenesis, boundary cells undergo a mesenchymal-to-epithelial transition, assembling an FN matrix along the boundary (Fig. 1A-G) (Crawford et al., 2003; Holley, 2007; Larsen et al., 2006). The somites form within the paraxial mesoderm, which is itself coated in FN matrix (Fig. 1H,I). Alignment of these superficial FN fibrils is regulated by non-canonical Wnt signaling; however, it is unknown how FN matrix is restricted ab initio to the surface of certain tissues (Davidson et al., 2004; Goto et al., 2005; Winklbauer, 1998). Initially, the FN matrix along the somite border is intermittent and does not appear as fibrillar as the matrix on the tissue surface, but the border matrix becomes increasingly dense and fibrillar during somite maturation before it is ultimately supplanted by a Laminin matrix (Crawford et al., 2003). Here we meld genetics and live imaging to investigate the in vivo regulation of Itgα5 and FN matrix assembly during zebrafish somite border morphogenesis.

MATERIALS AND METHODS

Zebrafish strains

Zebrafish were maintained using standard protocols (Nüsslein-Volhard and Dahm, 2002). Wild-type strains were Tübingen and TLF. Mutant alleles used were *integrin α5*: *bfe*^{thl30}, *bfe*^{tig453}; *deltaD*: *aei*^{tg249}; and *tbx24*: *fss*^{te314a} (Holley et al., 2000; Jülich et al., 2005; Nikaido et al., 2002; van Eeden et al., 1996). The *MZ itga5* mutant was generated by injection of *itga5* mRNA into embryos derived from *bfe*^{thl30} heterozygote incrosses, the embryos were raised and subsequently incrossed to identify homozygous adults. Since injected wild-type *itga5* mRNA would dissipate after a few days of development, the ability of these homozygous mutants to develop to adulthood indicates that *itga5* is not required past embryogenesis for zebrafish development, survival and reproduction.

mRNA and morpholino injections

Injections into 1-cell stage embryos were performed using standard protocols (Nüsslein-Volhard and Dahm, 2002). Itgα5 variants were made using overlap extension PCR, cloned into pCS2+ in frame with emerald GFP at the C-terminus and transcribed in vitro (Sp6, Ambion). Morpholino sequences for *itga5*, *fn1* (*natter*), *fn1b* (previously *fn3*) *ephrin B2a* and *epha4* (*epha4b*) have been described previously (Cooke et al., 2005; Jülich et al., 2005; Koshida et al., 2005; Trinh and Stainier, 2004).

[1]Department of Molecular, Cellular and Developmental Biology, Yale University, New Haven, CT 06520, USA. [2]Wellcome Trust Centre for Cell-Matrix Research, University of Manchester, Manchester M13 9PT, UK.

*Author for correspondence (scott.holley@yale.edu)

Accepted 30 June 2009

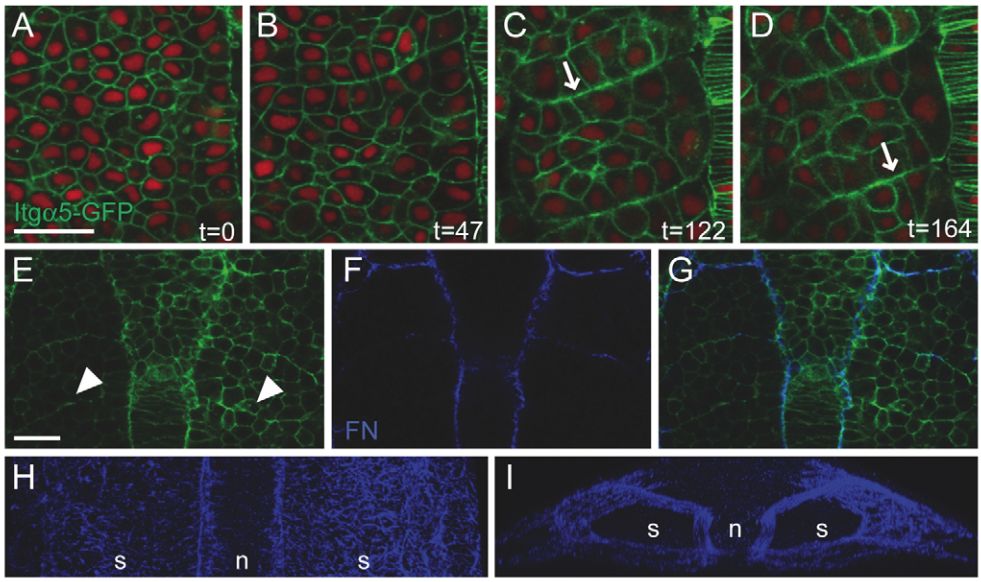

Fig. 1. Itgα5-GFP clustering and FN matrix assembly during somitogenesis in zebrafish. (**A-D**) Four time points (indicated in minutes) showing Itgα5-GFP localization during somite formation. Itgα5-GFP (green) is distributed along the cortex in mesenchymal presomitic cells (A) but clusters to the basal side of columnar border cells (B-D, arrows). Nuclei are red. (**E-G**) Itgα5-GFP (E), FN (F) and overlay (G). Nascent borders show Itgα5-GFP clustering (arrowheads in E) but no FN immunostaining. (**H**,**I**) Three-dimensional reconstruction showing FN matrix along the surface of the paraxial mesoderm. (A-H) Dorsal views, anterior is up. (I) Rotation of H showing a transverse view of the presomitic mesoderm, dorsal is up. Embryos are at the 8- to 10-somite (A-D,H,I) or 5- to 6-somite (E-G) stage. n, notochord; s, somites. Scale bars: 30 μm.

For BiFC constructs, the N-terminal 154 amino acids of Venus (up to VYIM) was fused in frame to the C-termini of Itgα5 and Itgα5^{FYLDD} via an 18 amino acid linker. The C-terminal 85 amino acids of Venus (starting with ADKQ) was fused in frame to the C-terminal end of zebrafish Itgβ1 via a six amino acid linker. All constructs were cloned into pCS2+, linearized with *Not*1, transcribed with Sp6 (Ambion) and injected at 100 ng/μl together with nlsRFP mRNA at the 1-cell stage; analysis was carried out at the 8- to 10-somite stage on the Zeiss LSM 510 confocal microscope with the same settings for all constructs (nlsRFP was used as reference).

Immunohistochemistry

Fibronectin localization was performed as previously described (Jülich et al., 2005). For GFP localization, embryos were fixed with 4% PFA/PBS, blocked with 10% BSA in PBSDT (PBS containing 1% DMSO, 0.1% Triton) and incubated with the GFP antibody (rabbit anti-GFP, A6455, Invitrogen) diluted 1:1000 in 1% BSA in PBSDT. The secondary antibody (Alexa Fluor 488 donkey anti-rabbit, Molecular Probes) was added at 1:200 in 1% BSA in PBSDT. For Epha4 Tyr602 antibody, embryos were fixed in 4% PFA/PBS, blocked in 2% blocking reagent (Roche), the primary antibody [EphA4 (Tyr-602), phospho-specific, EP2731 ECM Biosciences] was used at 1:100 dilution in 1% blocking reagent and the secondary antibody (Alexa Fluor 647 goat anti-rabbit, Invitrogen) was used at 1:200. For Ephrin B2 antibody, embryos fixed with 4% PFA/PBS, blocked in 1% blocking reagent (Roche) in PBSDT, primary antibody (anti-zfEphrin-B2, AF1088, R&D Systems) was used at 1:500 in 1% blocking reagent/PBSDT and secondary antibody (Alexa Fluor 647 goat anti-rabbit, Invitrogen) was used at 1:200 in 1% blocking reagent/PBSDT. For phalloidin staining, embryos were fixed with 4% PFA/PBS, incubated in PBS with 0.8% Triton X-100 for 6 hours, followed by overnight incubation at room temperature in Alexa Fluor 488 phalloidin (100 μM, Invitrogen) at 1:250 in PBS with 0.4% Triton X-100.

Production of recombinant soluble wild-type and mutant zebrafish α5β1-1

Recombinant soluble versions of zebrafish α5β1 containing the ectodomain of the α5 subunit fused to the hinge region and C_H2 and C_H3 domains of the human IgGg1 chain were made by cloning residues F33-Y982 (F1-Y950 in the mature sequence) of zebrafish α5 together with the leader sequence of a murine antibody (Kabat et al., 1987) into the pEE12.2hFc vector, essentially as previously described (Coe et al., 2001). Constructs containing the head region of β1-1 (Mould et al., 2006) [equivalent to the previously reported β1TR construct (Coe et al., 2001; Mould et al., 2002)] were made by cloning residues Q21-P475 of β1-1 (Q1-P455 in the mature sequence) fused with the murine antibody leader sequence into the pV.16hFc vector. Site-directed mutagenesis of the α5 subunit was carried out using the QuikChange II XL Kit (Stratagene) or by overlap extension PCR.

Chinese hamster ovary cells L761h variant (Coe et al., 2001) were maintained in Dulbecco's modified Eagle's medium supplemented with 10% fetal calf serum, 2 mM glutamine and 1% non-essential amino acids (growth medium). Six-well plates of subconfluent CHO-L761h cells were transfected with 1 μg of β1 construct and 1 mg of α5 construct per well using Lipofectamine Plus Reagent (Invitrogen). After 6 days, culture supernatants were harvested by centrifugation at 300 ***g*** for 5 minutes.

Formation of heterodimers was analyzed by western blotting of cell culture supernatants essentially as previously described (Valdramidou et al., 2008). In brief, aliquots of protein-A-purified cell culture supernatants were run on 3-8% SDS-PAGE gels under non-reducing conditions, transferred to nitrocellulose and blotted with anti-human Fc peroxidase conjugate (Stratech Scientific, Newmarket, UK). Bands were visualized using UptiLight Enhanced Chemiluminescence Reagent (Cheshire Biosciences, Chester, UK).

Solid-phase ligand-binding assays

The cell-binding domain fragment of zebrafish Fn1 (3Fn6-10 including EIIIB; residues T1093-T1632) was obtained by RT-PCR of RNA from zebrafish embryos 3 days post fertilization and cloned into the pCEP vector encoding a C-terminal FLAG tag. The cell-binding domain was produced by transient transfection of HEK 293 cells using Lipofectamine Plus Reagent (Invitrogen) under serum-free conditions. Fn1 fragment was purified from the cell culture medium using anti-FLAG M2 affinity gel (Sigma-Aldrich, Poole, UK) chromatography. The protein was biotinylated as previously described (Mould et al., 2002) using sulfo-LC-NHS biotin (Perbio, Chester, UK).

For ligand-binding assays, the binding of biotinylated Fn1 fragment (1 μg/ml) to Fc-captured recombinant Integrins was measured in solid-phase assays in the presence of 1 mM Mn^{2+} as previously described (Mould et al., 2002). To demonstrate whether ligand binding is specific, the effect of cyclic RGD peptide (ACRGDGSPCG 100 μg/ml) and EDTA (5 mM) on protein binding was tested.

Cell transplantation

Mosaic embryos were generated using standard methods (Nüsslein-Volhard and Dahm, 2002). Donor embryos were labeled with 2% rhodamine dextran. Donor and host embryos were manually dechorionated in E2 buffer. Mosaic host embryos were allowed to develop until 10-12 somites, assayed under a fluorescent dissecting scope for morphological boundary formation and fixed in 4% PFA/PBS for further analysis.

Image acquisition and processing

Confocal and time-lapse images were collected on a Zeiss LSM 510 microscope. DIC images were acquired on a Zeiss Axioskop microscope. Time-lapse datasets were processed using Imaris (Bitplane) to export individual time points, Adobe Photoshop CS3 was used to crop images and reduce file size and Quicktime Pro was used to assemble the image stacks into time-lapse movies. Three-dimensional reconstructions were made using Imaris. Individual confocal images were processed using ImageJ. Figures were assembled using Adobe Illustrator CS3.

RESULTS

Initiation of Itgα5 clustering is independent of FN binding

We previously found that zebrafish Itgα5-GFP, in which GFP is tagged to the cytoplasmic tail of Itgα5, completely rescues *itga5*$^{-/-}$ embryos (Jülich et al., 2005). Itgα5-GFP is expressed on the cell cortex of mesenchymal presomitic mesoderm (PSM) cells, where FN is also expressed, yet no FN matrix is assembled within the PSM. In nascent somite boundary cells of live embryos, we observed basal clustering of Itgα5-GFP concomitant with the earliest indication of border morphogenesis (Fig. 1A-D; see Movie 1 in the supplementary material). Visualization of Itgα5-GFP and the FN matrix with immunohistochemistry showed Itgα5-GFP clustering prior to FN matrix assembly (Fig. 1E-G). Thus, Itgα5-GFP clusters along the basal side of the somite border and shortly thereafter FN matrix is observed. During this transition, we conclude that Itgα5-dependent FN matrix assembly is initiated and thus that Itgα5 has become activated. By 'activated' we mean that the matrix assembling function of Itgα5 becomes elevated and that this elevation is concomitant with the polarized clustering of Itgα5-GFP. Because the clustering precedes the appearance of FN matrix along the somite boundary, we hypothesize that the clustering is driven by 'inside-out' signaling. If this is correct, then a form of Itgα5 that cannot bind ligand should also cluster during the initiation of border morphogenesis.

We generated a series of Itgα5 variants with mutations in key residues previously shown or predicted to be necessary for ligand binding (Fig. 2A). The α5β1 heterodimer binds to two domains in FN: the canonical RGD sequence, which is the primary binding site, is in the tenth type-III FN repeat, whereas the synergy site resides in the ninth type-III FN repeat (Wierzbicka-Patynowski and Schwarzbauer, 2003). The residues that recognize the RGD domain reside in the β Integrin subunit and in loops within the β-propeller domain of the α subunit. In particular, the residue equivalent to D224 in the αV subunit forms a salt bridge with arginine in the RGD sequence (Xiong et al., 2002). Mutation of the residue equivalent to F183 has been reported to eliminate RGD binding by human α5β1

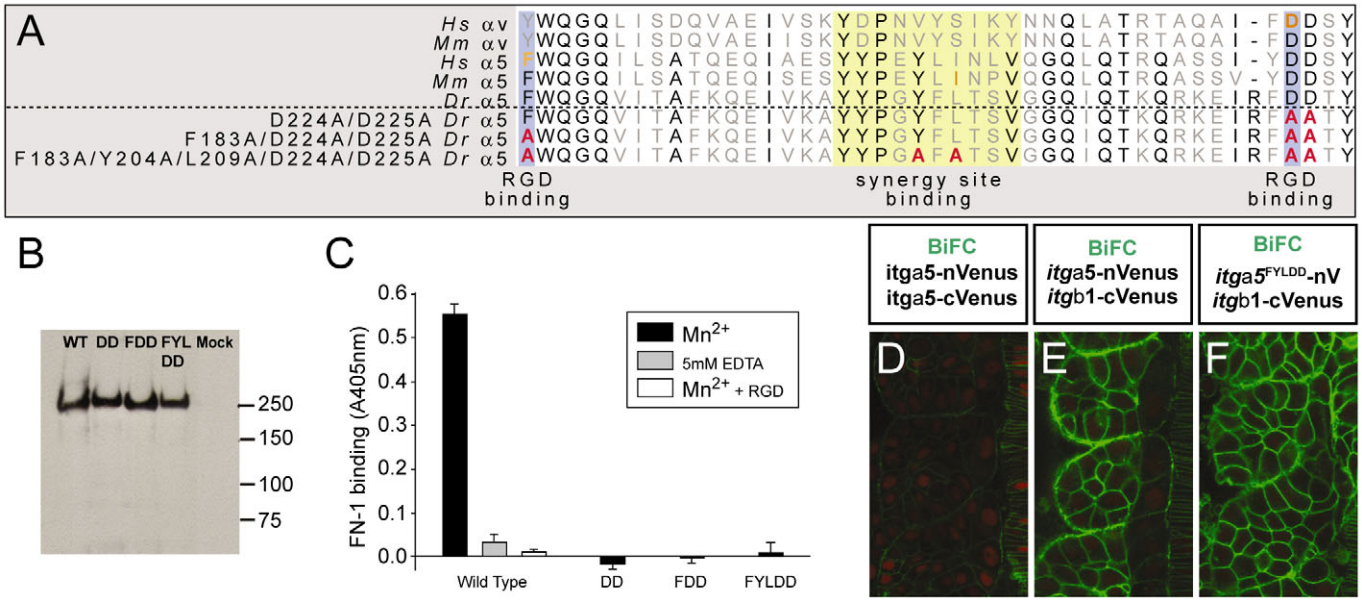

Fig. 2. Ligand-binding-deficient variants of Itgα5. (**A**) An alignment of a portion of the β-propeller domain of human (*Hs*), mouse (*Mm*) and zebrafish (*Dr*) Integrin α5 and αV. Residues known to be necessary for RGD binding (blue) and synergy site binding (yellow) are indicated. The orange residues have been analyzed experimentally in the corresponding Integrin. The sequences of the modified zebrafish Itgα5 are shown with the altered residues in red. (**B**) Western blotting of wild-type (WT) and mutant (DD, FDD and FYLDD) recombinant-soluble α5β1-Fc Integrins, showing that in each case a heterodimer is formed of ~240 kDa. This band is not observed in proteins purified from the supernatants of mock-transfected cells. (**C**) Ligand-binding assay. Binding of a recombinant fragment of zebrafish Fn1 to wild-type or mutant (DD, FDD and FYLDD) α5β1-1-Fc was measured in a solid-phase assay in the presence of 1 mM Mn^{2+} to activate the Integrin (black bars). To demonstrate specificity of Fn1 binding to the wild-type Integrin, the interaction was also measured in the presence of cyclic RGD peptide (white bar) or 5 mM EDTA (gray bar). (**D-F**) BiFC demonstrates that the mutant Itgα5^{FYLDD} forms a heterodimer with Itgβ1 on the cell cortex in vivo. Negative (D) and positive (E) controls are also shown. Anterior is up and medial is to the right.

(Irie et al., 1995; Mould et al., 2003). Within the synergy-site-binding domain, we made concomitant Y204A/L206A substitutions. Y204 is highly conserved, and a Y204N mutation is responsible for the craniofacial defect of a zebrafish *integrin α5* mutant (Crump et al., 2004). L206 is in the same position as the isoleucine in mouse and human integrin α5. Mutation of this tyrosine or isoleucine to alanine in human integrin α5 reduces synergy site binding by 5- and 200-fold, respectively (Mould et al., 2003). Based on these studies, we made three Integrin α5 variants that were extensively characterized: D224A/D225A (Itgα5^{DD}), F183A/D224A/D225A (Itgα5^{FDD}) and F183A/Y204A/L206A/D224A/D225A (Itgα5^{FYLDD}).

To determine whether these mutations in fact ablated ligand binding, we performed in vitro binding assays. We generated recombinant soluble versions of the zebrafish Integrins containing the complete extracellular domain of the α5 subunit and the headpiece of the β1-1 subunit (Mould et al., 2006) fused to the hinge region, the C_H2 and C_H3 domains of the human IgGγ1 chain. These constructs were chosen because expression of the head and leg regions of the α subunit together with the head region of the β subunit is sufficient to create a constitutively active Integrin (Mould et al., 2005). Recombinant wild-type and mutant Integrins were partially purified from the cell culture medium using Protein-A sepharose and the formation of heterodimers was examined by western blotting (Fig. 2B). In each case, a predominant band at ~240 kDa was observed, corresponding to the expected mass of an α,β-Fc heterodimer. A recombinant fragment of zebrafish Fn1 containing the synergy and RGD binding sites was produced. Interaction of this fragment with the recombinant Integrins was examined in solid-phase assays (Fig. 2C). The fragment bound well to the wild-type Integrin, but no binding of the fragment to the Itgα5^{DD}, Itgα5^{FDD} or Itgα5^{FYLDD} variants was observed.

To determine whether these Itgα5 variants form heterodimers with Itgβ1 in vivo, we performed bimolecular fluorescence complementation (BiFC) (Kerppola, 2008; Saka et al., 2008). Itgα5 and Itgα5^{FYLDD} were tagged at their C-termini with the N-terminal fragment of Venus YFP (Itgα5-nVenus and Itgα5^{FDDYL}-nVenus, respectively). A second Itgα5 construct included a C-terminal tag of C-terminal fragment of Venus (Itgα5-cVenus). Itgβ1 was tagged at its C-terminus with the C-terminal fragment of Venus (Itgβ1-cVenus). Coexpression of Itgα5-nVenus and Itgα5-cVenus produced weak fluorescence on the cell cortex, presumably owing to clustering of Integrin heterodimers in the plasma membrane and/or aggregation of Integrins in lipid microdomains (Fig. 2D). Coexpression of Itgα5-nVenus and Itgβ1-cVenus produced strong fluorescence on the cell cortex (Fig. 2E). Similarly, expression of Itgα5^{FDDYL}-nVenus and Itgβ1-cVenus produced strong fluorescence on the cell cortex (Fig. 2F). Since each BiFC combination was imaged with the same confocal settings, the increase in signal seen when the α and β subunits were coexpressed, as compared with when the two α subunits were coexpressed, should be due to heterodimerization. Consistent with the western blot data (Fig. 2B), these experiments indicate that the modifications of the ligand-binding domain in Itgα5 do not perturb its formation of a heterodimer with Itgβ1.

Using mRNA injection, we tested the ability of these *itga5* variants to rescue the segmentation defect of the *itga5* mutant, as assayed by morphological segmentation and FN matrix assembly. Each variant contains a C-terminal GFP tag. In contrast to the injection of mRNA encoding the wild-type *itga5* (Jülich et al., 2005), we found that the variants represent an allelic series, in that *itga5*^{DD} and *itga5*^{FDD} failed to rescue the segmentation defect and *itga5*^{FYLDD} failed to rescue and was strongly antimorphic (Fig. 3A-F,H,J,M,N). The antimorphic activity manifests as an enhanced mutant phenotype, presumably owing to competition with maternally supplied wild-type Itgα5 for heterodimerization with Itgβ1 (Fig. 3, compare C with F and M with N). The antimorphic activity of the *itga5*^{FYLDD} allele was also strong enough to cause a head defect in injected wild-type sibling embryos (see Fig. S1 in the supplementary material). This head defect is seen in the *itga5* mutants and exhibits a greater sensitivity to loss of *itga5* than somitogenesis.

These ligand-binding-deficient Integrins were assayed for their ability to cluster along the somite boundary in the absence of endogenous *itga5*. Despite their inability to mediate FN matrix assembly, each of the Itgα5-GFP variants transiently clustered along nascent somite boundaries, supporting the hypothesis that clustering is instigated by inside-out signaling (Fig. 3A,I,K,O-Q). However, the capacity to bind FN is required for FN matrix assembly (Fig. 3H,J,N), stabilization of the somite border and maintenance of basal clustering of Itgα5 (Fig. 3P,Q). To exclude the possibility that small amounts of residual maternal Itgα5 might initiate clustering of the mutant Itgα5-GFP, we generated maternal-zygotic (*MZ*) *itga5*$^{-/-}$ embryos. The *MZ itga5*$^{-/-}$ embryos lack all Itgα5 and have enhanced morphological defects (Fig. 3G) and loss of FN matrix (Fig. 3L) but still make posterior somites. Time-lapse analysis of *MZ itga5*$^{-/-}$ embryos expressing Itgα5^{FYLDD}-GFP during anterior trunk somitogenesis (Fig. 3P,Q; see Movie 2 in the supplementary material) shows that the ability to bind FN is not required for initial Itgα5^{FYLDD}-GFP clustering. However, ligand binding is required to stabilize the clustering.

Activated unbound Itgα5β1 has been observed in focal contacts of fibroblasts in 2D culture, but translocation of the Integrin in this context was FN-dependent (Pankov et al., 2000). Our results are reminiscent of clustering of activated unbound Itgα5β1 along the leading edge of lamellae and filopodia in cultured migrating fibroblasts (Galbraith et al., 2007).

FN dimers are readily available for assembly into an ECM

Our clustering analysis suggests that formation of FN matrix along the somite boundary is regulated by inside-out signaling. To further examine Itgα5 regulation, we made a series of genetic mosaics via cell transplantation (Fig. 4A). For most of the transplantation experiments, we used the *fused somites* (*fss*) mutant as the genetic background because these embryos do not form somite borders, allowing us to attribute any border formation to our experimental manipulation (van Eeden et al., 1996). *fss* embryos are mutant for the transcription factor Tbx24 and, although the mutants fail to express a number of genes normally transcribed in a segmental pattern within the somites, they do express *itga5*, *itgb1*, *fn1* and *fn1b*, and make FN matrix on the surface of the paraxial mesoderm (Jülich et al., 2005; Koshida et al., 2005; Nikaido et al., 2002; Trinh and Stainier, 2004). Using genetic mosaics, we first addressed whether secretion or the availability of FN is limiting. To eliminate all FN, we injected antisense morpholinos (*fn1/1b*mo) against the two zebrafish fibronectin genes *fn1* and *fn1b* (*n*=13) (Fig. 4C,D). We previously showed that knockdown of these two genes results in a severe truncation of the posterior body (Jülich et al., 2005). We created mosaics in which the donor clones lack FN but express *itga5*-GFP, whereas the host cells express FN but not *itga5* as a consequence of anti-*itga5* morpholino injection. In 89% of clones, we observed a morphological boundary around the clone (*n*=44) (Fig. 4B,E,F). We found that FN matrix was assembled along the

border of 68% of the clones (*n*=22) (Fig. 4G). We repeated these experiments using *fn1/1b*mo;*itga5-GFP*;wild-type donors transplanted into *itga5*mo;*deltaD*$^{-/-}$ hosts, which also lack somite boundaries (Jülich et al., 2005). In this second genetic background, we again observed borders around 94% of clones (*n*=80) (Fig. 4B) and FN matrix around 58% of these clones (*n*=64). Together, these genetic mosaic experiments show that FN dimers secreted by the host cells can be converted into a matrix by the Itgα5-expressing donor cells, indicating that FN dimers are readily available for assembly into an ECM. Cumulatively, the data suggest that inside-out signaling might initiate de novo assembly of the FN matrix along the somite boundary.

Integrins expressed on adjacent cells reciprocally inhibit Integrin clustering and ECM assembly

Next, we addressed why morphological borders and FN matrix form in these genetic mosaics. The above mosaics comprised *itga5*-expressing clones with hosts lacking *itga5*. We simplified the mosaics by only manipulating *itga5* and leaving *fn1/1b* unchanged. In mosaics of *itga5*mo;*fss* donors and *itga5-GFP*;*fss* hosts, we observed morphological borders along 77% of clones (*n*=69) (Fig. 4B), of which 82% assembled FN along the boundary (*n*=33) (Fig. 4H-J) and 80% had basal Actin belts mimicking somite boundaries (*n*=15) (Fig. 4K) (Barrios et al., 2003). We note that transplantation of *fss*$^{-/-}$ cells into *fss*$^{-/-}$ embryos leads to border formation around 23% of the clones, even though *fss*$^{-/-}$ embryos do not normally form any borders (Fig. 4B). Thus, the transplantation itself appears to lead to morphological fissure between donor and host cells in about a quarter of mosaic embryos. Other control mosaics formed borders in no more than 31% of cases (Fig. 4B).

The increase in the efficiency of border and matrix formation when, counterintuitively, Itgα5 is missing in the donor or host suggests that Itgα5 non-cell-autonomously inhibits Itgα5 on adjacent cells, preventing Integrin clustering and the spontaneous conversion of FN dimers into a matrix. This Itgα5-dependent repression is revealed when cells expressing Itgα5 are juxtaposed to cells that do not have Itgα5, relieving the inhibition along the interface and leading to Integrin clustering and FN matrix assembly.

A

itga5 Variant	% somite defects; (# of embryos); *# of experiments*	Antimorphic activity?	Itgα5-GFP Clustering?
itga5^{DD}	28%; (n=82); *4 exp.*	no	yes
itga5^{FDD}	26%; (n=686); *9 exp.*	no	yes
itga5^{FYLDD}	28.5%; (n=488); *8 exp.*	yes	yes

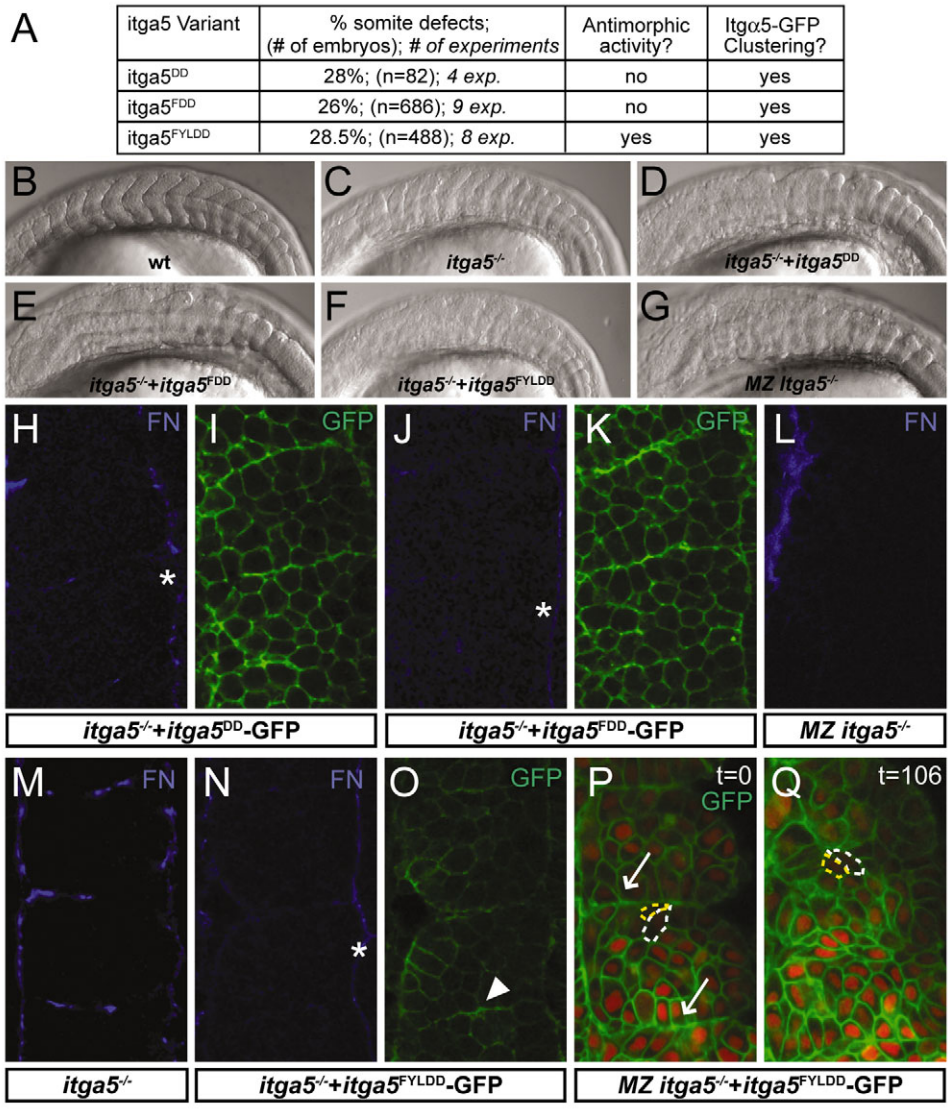

Fig. 3. Initial clustering of Itgα5-GFP is independent of FN. (**A**) In vitro transcribed mRNAs encoding Itgα5-GFP variants were injected at 250 ng/μl into zebrafish embryos derived from Itgα5$^{-/+}$ parents. Injected embryos were assayed morphologically for somite defects, for antimorphic activity and for Itgα5-GFP clustering. (**B-G**) Lateral views of the trunk somites in 14- to 18-somite stage embryos. Anterior is left. (B) A wild-type (wt) embryo. (C) An *itga5*$^{-/-}$embryo. Somitogenesis in *itga5*$^{-/-}$ is not rescued by injection of mRNA encoding Itgα5^{DD}-GFP (D), Itgα5^{FDD}-GFP (E) or Itgα5^{FYLDD}-GFP (F). The *itga5*$^{-/-}$ embryo in C is an uninjected sibling of the embryo in F. Note that the morphological somite defects are enhanced by Itgα5^{FYLDD} expression. (G) Loss of maternal *itga5* enhances the zygotic *itga5*$^{-/-}$ phenotype; however, posterior trunk and tail somites form in these embryos. (**H-O**) Embryos at the 6- to 8-somite stage. Itgα5^{DD}-GFP does not rescue segmental FN assembly in *itga5*$^{-/-}$ embryos (H) but clusters along nascent borders (I). Similarly, Itgα5^{FDD}-GFP does not rescue segmental FN assembly in *itga5*$^{-/-}$ embryos (J) but clusters along nascent borders (K). (L) *MZ itga5*$^{-/-}$ embryos lack segmental FN. FN localization in *itga5*$^{-/-}$ (M) and an *itga5*$^{-/-}$ embryo injected with Itgα5^{FYLDD} (N). (O) Itgα5^{FYLDD}-GFP localization in the embryo shown in N. Note that the FN-matrix defects are enhanced by injection of Itgα5^{FYLDD}, with matrix only forming along the surface of the paraxial mesoderm (asterisks). Nonetheless, Itgα5^{FYLDD}-GFP clustering is observed (arrowhead). (**P**,**Q**) Two time points (indicated in minutes) of Itgα5^{FYLDD}-GFP localization in an 8- to 10-somite stage embryo lacking maternal and zygotic *itga5* (*MZ itga5*$^{-/-}$). A functional ligand-binding domain is not necessary for initial clustering (arrows) but is required to maintain clustering. For reference, the same two cells are outlined in yellow and white. (H-Q) Anterior is up.

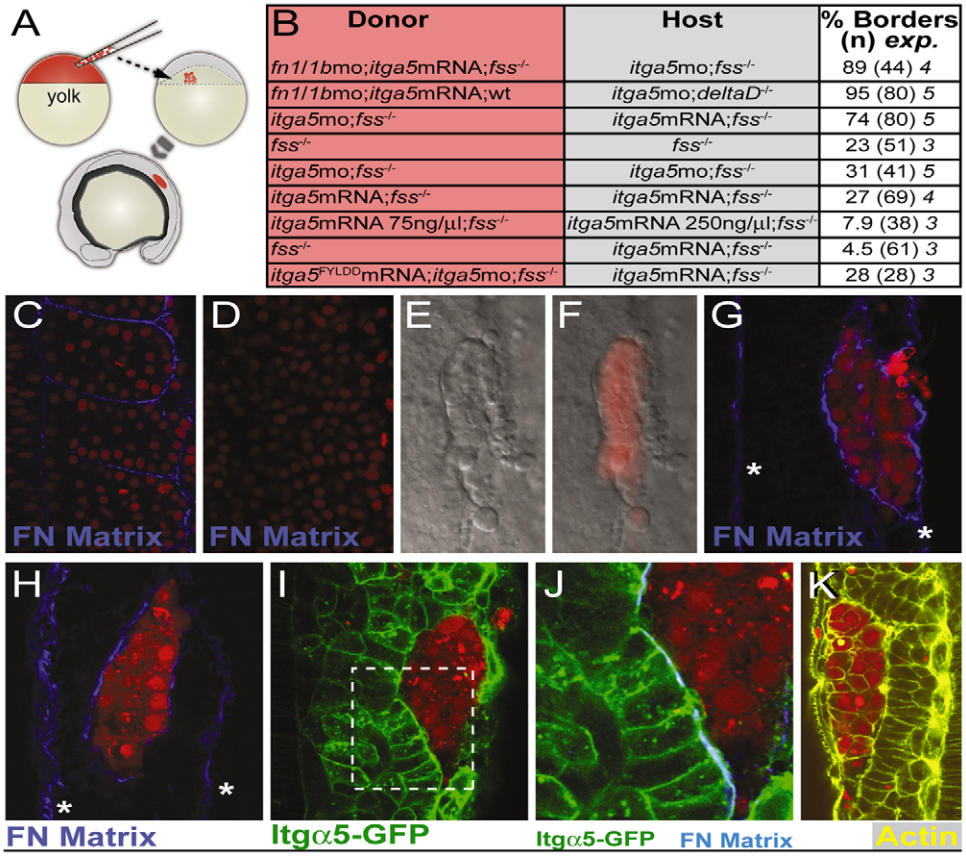

Fig. 4. Itgα5 non-cell-autonomously inhibits clustering and FN matrix assembly. (**A**) Genetic mosaics were made by transplanting labeled cells (red) from the blastula of a donor zebrafish embryo into the late blastula of an unlabeled host embryo. The chimeras were later analyzed for morphological border formation, greater than three cell diameters in length, around clones within the paraxial mesoderm. (**B**) Summary of the genetic mosaic experiments. Donor and host genotypes and treatments are indicated. The percentage of clones with borders, the total number of embryos examined and the number of experiments are displayed. (**C**,**D**) FN matrix (C) is eliminated by injection of *fn1/fn1b* morpholinos (D). FN matrix is blue and nuclei are red. (**E**,**F**) DIC image (E) and composite of a clone (F, red) with a border separating it from the host cells. (**G**) FN matrix forms along a clone lacking *fn* but expressing *itga5* within a host lacking *itga5* but expressing *fn*. Asterisks indicate FN matrix along the medial and lateral surfaces of the paraxial mesoderm. (**H**) FN matrix forms along a clone lacking *itga5* within a host expressing *itga5*. (**I**) In mosaics of the same genotype as in H, Itgα5-GFP clusters along the clone. (**J**) The boxed region in I shown with FN matrix (blue) colocalizing with the clustered Itgα5-GFP. Note the columnar morphology of the host border cells. (**K**) Actin belts are seen along the clone borders. (C-K) Anterior is up.

To probe the mechanism of the non-cell-autonomous trans-inhibition, we performed a cell transplantation experiment in which the donor cells only express Itgα5^{FYLDD}, whereas the hosts express wild-type Itgα5. Itgα5^{FYLDD} was able to suppress FN matrix assembly by the host Itgα5, indicating that non-cell-autonomous trans-inhibition does not require Integrin-FN interaction (Fig. 4B). We observe this non-cell-autonomous trans-inhibition in three genetic backgrounds comprising mosaics in which either the donor or host is *itga5*-deficient (Fig. 4B). The non-cell-autonomous trans-inhibition observed here appears to differ from cell-autonomous ‘trans-dominant’ Integrin inhibition involving competition by the Integrin cytoplasmic tails for Talin, a soluble component of focal adhesions that mediates both interactions with the cytoskeleton and Integrin signaling (Calderwood et al., 2004).

Eph/Ephrin signaling acts upstream of Integrin clustering and ECM assembly

Our data suggest that Itgα5 on adjacent cells inhibits the spontaneous assembly of ubiquitous FN dimers into an ECM. During somite border morphogenesis, this inhibition is apparently relieved when Itgα5 is activated by inside-out signaling. The question remains, what signal initiates Integrin activation to override the trans-inhibition? A good candidate is Eph/Ephrin signalling, which modulates adhesion via Integrins in other biological contexts (Pasquale, 2008). The receptor tyrosine kinase Epha4 and its ligand Ephrin B2a are expressed in the anterior and posterior halves of nascent somites, respectively (Durbin et al., 1998). The somite border thus forms at the interface between the *epha4* and *ephrin B2a* expression domains. Upon ligand binding, tyrosine residues on the cytoplasmic domain of Eph are phosphorylated (Pasquale, 2008). Thus to visualize active Epha4 signaling, we used polyclonal antisera against phospho-tyrosine 602 of human EPHA4. The region around this tyrosine is identical to zebrafish Epha4. We observed immunostaining along the somite borders and in the notochord, where Epha4 is highly expressed (Fig. 5A). Thus, EphA4 signaling is active in the region where Itgα5-GFP clusters. Injection of a morpholino targeting *epha4* strongly reduces or eliminates (63% and 37%, respectively; n=8) the specific notochord and somite boundary staining (Fig. 5B). Although this morpholino can cause a hindbrain boundary defect, we see no obvious somite phenotype in injected

wild-type embryos and no strong exacerbation of the boundary defect when injected into *itga5*$^{-/-}$ embryos (data not shown) (Cooke et al., 2005). Ephrin B2a levels are highest in the posterior half of each somite (Fig. 5C). Injection of an *ephrin B2a* morpholino (Cooke et al., 2005) completely eliminates Ephrin B2a expression (*n*=12; Fig. 5D). Although this morpholino does not cause a somite defect when injected into wild-type embryos, it does exacerbate the somite defect when injected into *itga5*$^{-/-}$ embryos (Koshida et al., 2005).

Activated Epha4 can be seen along the transient borders formed in *MZ itga5*$^{-/-}$ embryos, indicating that *itga5* is not required for Epha4 activation (71%, *n*=7; Fig. 5E). We expressed Itgα5^{FYLDD} in *MZ itga5*$^{-/-}$ embryos and found that Epha4 activation colocalizes with transient ligand-independent clustering of Itgα5^{FYLDD} (86%, *n*=7; Fig. 5F-H). Injection of *ephrin B2a* morpholino into *MZ itga5*$^{-/-}$ embryos eliminates both Epha4 activation (*n*=6) and Itgα5^{FYLDD}-GFP clustering (*n*=40; Fig. 5I,J). Thus, ligand-independent Itgα5 clustering colocalizes with active Eph/Ephrin signaling and is dependent upon *ephrin B2a*.

To determine whether Eph/Ephrin signaling is sufficient to induce Itgα5 clustering and FN matrix formation, we performed a series of genetic mosaic experiments. *epha4* expression is lost in *fss*$^{-/-}$ embryos and there is ubiquitous expression of *ephrin B2a*. Transplantation of *ephA4*-expressing cells into *fss* embryos led to border formation along 83% of clones (*n*=71; five experiments; Fig. 5K-M) (Barrios et al., 2003; Durbin et al., 2000). Furthermore, we find that Eph/Ephrin signaling can induce basal Actin belts (86%; *n*=14; Fig. 5N). In these mosaics, both the donor and host express Itgα5-GFP. We observed that Eph/Ephrin signaling could induce Itgα5-GFP clustering (42%; *n*=12; Fig. 5L,M) and FN matrix assembly (91%; *n*=11; Fig. 5O,P). We also performed these experiments without the expression of Itgα5-GFP, but in the presence of endogenous Itgα5, and observed borders along 69% of clones (*n*=55; five experiments) and FN matrix around 80% of clones (*n*=15). We next used a truncated Epha4 in which the kinase domain has been deleted (dnEpha4) (Barrios et al., 2003; Davis et al., 1994; Xu et al., 1995). Thus, the dnEpha4 can induce reverse signaling by Ephrin B2a, but it cannot transduce a forward signal in the dnEpha4-expressing cells. *dnepha4*;*fss*$^{-/-}$ clones in *fss*$^{-/-}$ hosts induced borders in 77% of cases (*n*=48; three experiments; Fig. 5Q-S). *ephrin B2a*-expressing host cells exhibited Itgα5-GFP clustering along the 83% of clones (*n*=12; Fig. 5Q-S) and 81% of clones were bound by FN matrix (*n*=27; Fig. 5R,S). These data indicate that Ephrin B2a reverse signaling is sufficient to cause Itgα5 clustering and FN matrix assembly.

DISCUSSION

The interplay between inside-out activation, initiated by Eph/Ephrin signaling, and Itgα5 non-cell-autonomous trans-inhibition would insure the segmental production of ECM during somitogenesis

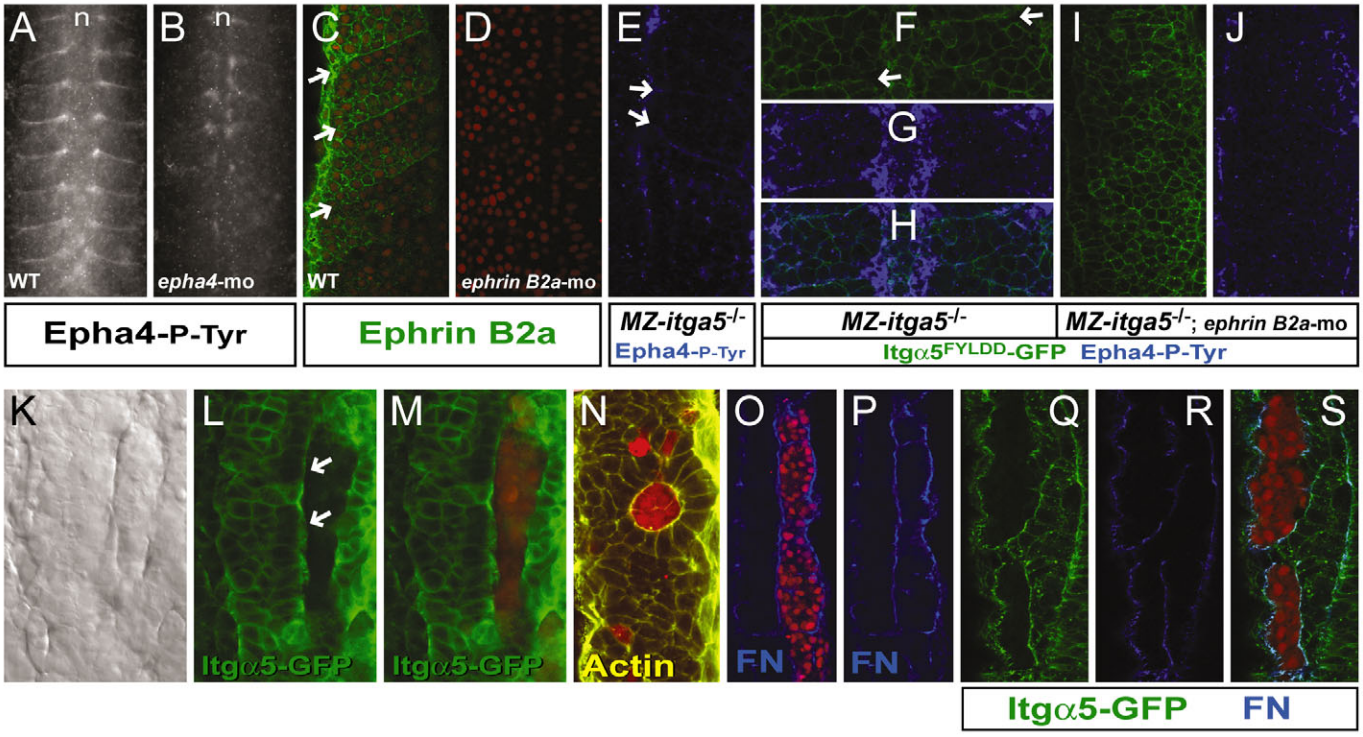

Fig. 5. Eph/Ephrin signaling can induce Itgα5 clustering and FN matrix assembly. (**A-D**) Phosphorylated Epha4 (Epha4-P-Tyr) localizes to somite boundaries and the notochord (n) in wild-type zebrafish embryos (A) but is substantially reduced in *epha4* morpholino-injected embryos (B). Ephrin B2a (green) is expressed in a graded fashion in the posterior somites (arrows) of wild-type embryos (C) but is absent in *ephrin B2a* morpholino-injected embryos (D). Nuclei are red. (**E**) Epha4-P-Tyr localizes to transient somite boundaries (arrows) in *MZ itga5*$^{-/-}$ embryos. (**F-H**) Epha4-P-Tyr blue) colocalizes with ligand-independent Itgα5^{FYLDDD}-GFP clustering (arrows) in *MZ itga5*$^{-/-}$ embryos. (**I,J**) Morpholino knockdown of *ephrin B2a* abolishes ligand-independent Itgα5^{FYLDD}-GFP clustering. (**K-M**) *epha4*-expressing clones (red) in a host with no *epha4* but with broadly expressed *ephrin B2a*. Eph/Ephrin signaling can induce a border (K) and Itgα5-GFP clustering (L,M) around the donor clone. Note that Itgα5-GFP in the host cells is largely localized to the border with the clone (arrows), not along the lateral cell cortices. (**N**) A rosette with polarized host cells surrounding an *epha4*-expressing clone. Actin fibrils concentrate along the 'basal' surface of the host cells, similar to polarization along somite boundaries. (**O**,**P**) FN matrix is assembled around the *epha4*-expressing clone. (**Q-S**) A *dnepha4*-expressing clone (red) induces Itgα5-GFP clustering and FN matrix assembly. C,D,H,M,N,O,S are overlays.

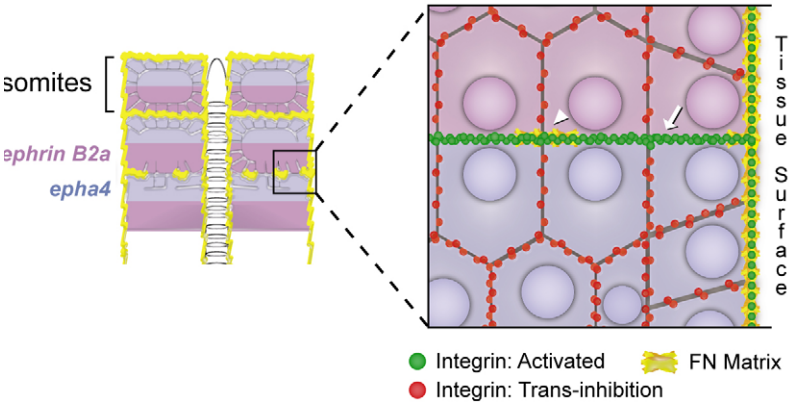

Fig. 6. A model for the control of Itgα5 activation and FN matrix assembly along somite borders and tissue surfaces in zebrafish. Itgα5 engages in non-cell-autonomous trans-inhibition within the paraxial mesoderm (red), but this inhibition is relieved along the tissue surface allowing the coating of the paraxial mesoderm with an FN matrix (yellow). Along the nascent somite border, Itgα5 clustering (green) occurs along the interface of *ephrin B2a* (purple) and *epha4* (blue) expression domains, where Epha4 activation is highest. Itgα5 clustering (arrow) precedes FN matrix assembly (arrowhead) along the forming border.

(Fig. 6). In this model, segmental stripes of Epha4 and Ephrin B2a initiate inside-out signaling, thereby overriding Integrin inhibition and leading to Itgα5 clustering and matrix assembly along the nascent somite border (Fig. 6). This inside-out activation does not involve an elimination of Itgα5 on one side of the border (Fig. 1A-D). Our mosaics detailed in Fig. 4, in which FN matrix forms in the absence of *epha4*, at the interface between Itgα5-expressing and non-expressing cells, show that loss of trans-inhibition is epistatic to loss of inside-out signaling. In other words, lack of trans-inhibition bypasses the need for Eph/Ephrin in initiating Itgα5 clustering and FN matrix assembly. This observation suggests that Eph/Ephrin-induced inside-out signaling regulates trans-inhibition, rather than vice versa. The fact that Itgα5^{FYLDD} can repress matrix assembly by wild-type Itgα5 on adjacent cells shows that the ability to bind ligand is not required for Itgα5-dependent inhibition of matrix assembly. It also indicates that derepression of non-cell-autonomous trans-inhibition via loss of Itgα5 is not due to indirect effects of loss of Itgα5 signaling or adhesion because Itgα5^{FYLDD} restores repression without rescuing 'normal/canonical' Itgα5 function.

Our data indicate that reverse signaling by Ephrin B2a is sufficient to initiate Itgα5 clustering and induce FN matrix assembly. *ephrin B2a* morpholino injection into *MZ itga5*$^{-/-}$ embryos showed that Itgα5 clustering depends upon *ephrin B2a*, but we do not know whether this requirement is for forward signaling, reverse signaling or both. Genetic experiments in mice appear to indicate that murine somitogenesis is dependent only upon ephrin B2 forward signaling (Davy and Soriano, 2007). We were not able to determine whether forward signaling by Eph is sufficient to cause Itgα5 clustering and FN matrix assembly because we could not definitively block all reverse signaling via the *ephrin B2a* morpholino or via a truncated dominant-negative form of Ephrin B2a (Barrios et al., 2003). *ephrin A1* and *ephrin B2b* are also expressed in the somites and thus may compensate for the loss of *ephrin B2a* (Barrios et al., 2003; Durbin et al., 1998).

It is possible that reverse signaling by Ephrin B2a could drive normal boundary formation in the absence of forward Eph signaling. We note that the posterior-most cells of each somite that express the highest levels of Ephrin B2a polarize more dramatically and rapidly than the *epha4*-expressing cells on the other side of the border. In principle, contact-mediated inhibition leading to a reduction in cell-cell (Cadherin-mediated) adhesion between Ephrin- and Eph-expressing cells could result in derepression of non-cell-autonomous trans-inhibition by separating the Itgα5 on adjacent cells. In this way, Ephrin-induced Itgα5 clustering in the Epha4-expressing cell could be independent of Epha4 forward signaling. One can take this idea one step further. In theory, Eph/Ephrin contact-mediated repulsion could lead to Itgα5 activation on both sides of the somite border by simply causing the separation of opposing border cells, leading to derepression of the Itgα5 trans-inhibition. In this way, initial Integrin activation may be ligand independent but may not involve direct signaling to Itgα5 by either Eph or Ephrin signaling.

Itgα5 forward signaling may feedback on Eph/Ephrin signaling or other regulators of cell adhesion or cell polarity during somite border morphogenesis. Immunohistochemical analysis suggests coordinated changes in focal adhesions and adherens junctions during zebrafish somitogenesis (Crawford et al., 2003). Moreover, FN matrix forms at the interface of cells with disparate levels of Cadherin expression (Dzamba et al., 2009). Indeed, Itgα5-dependent non-cell-autonomous inhibition of matrix formation might require Cadherins or other regulators of cell-cell adhesion.

Finally, our data might explain the presence of ECM along the outer surface of the paraxial mesoderm, as surface cells express Itgα5 and lack strong contact with cells in adjacent tissues. This arrangement would lead to the observed Integrin clustering along the superficial edge of surface cells and ECM assembly along the exterior of the paraxial mesoderm (Fig. 6). Thus, matrix production might be an intrinsic property of the tissue rather than being dependent upon inductive signals arising in the heterogeneous environments present along the dorsal, ventral, medial and lateral edges of the paraxial mesoderm. Such a mechanism utilizing surface derepression of Integrin-dependent inhibition of matrix assembly might be generally used to self-organize and maintain tissue boundaries.

Acknowledgements
We thank Jim Smith for the Venus BiFC constructs; Stephen Wilson for the *epha4* and *ephrin B2a* plasmids; Joe Wolenski for help with the microscopy; and David Calderwood and members of the lab for comments on the manuscript. Research support was provided by a Research Scholar Grant from the American Cancer Society.

Supplementary material
Supplementary material for this article is available at
http://dev.biologists.org/cgi/content/full/136/17/2913/DC1

References
Alon, R. and Feigelson, S. (2002). From rolling to arrest on blood vessels: leukocyte tap dancing on endothelial integrin ligands and chemokines at sub-second contacts. *Semin. Immunol.* **14**, 93-104.
Askari, J. A., Buckley, P. A., Mould, A. P. and Humphries, M. J. (2009). Linking integrin conformation to function. *J. Cell Sci.* **122**, 165-170.
Barrios, A., Poole, R. J., Durbin, L., Brennan, C., Holder, N. and Wilson, S. W. (2003). Eph/Ephrin signaling regulates the mesenchymal-to-epithelial transition of the paraxial mesoderm during somite morphogenesis. *Curr. Biol.* **13**, 1571-1582.
Bokel, C. and Brown, N. H. (2002). Integrins in development: moving on, responding to, and sticking to the extracellular matrix. *Dev. Cell* **3**, 311-321.

Calderwood, D. A., Tai, V., Di Paolo, G., De Camilli, P. and Ginsberg, M. H. (2004). Competition for talin results in trans-dominant inhibition of integrin activation. *J. Biol. Chem.* **279**, 28889-28895.
Coe, A. P., Askari, J. A., Kline, A. D., Robinson, M. K., Kirby, H., Stephens, P. E. and Humphries, M. J. (2001). Generation of a minimal alpha5beta1 integrin-Fc fragment. *J. Biol. Chem.* **276**, 35854-35866.
Cooke, J. E., Kemp, H. A. and Moens, C. B. (2005). EphA4 is required for cell adhesion and rhombomere-boundary formation in the zebrafish. *Curr. Biol.* **15**, 536-542.
Crawford, B. D., Henry, C. A., Clason, T. A., Becker, A. L. and Hille, M. B. (2003). Activity and distribution of paxillin, focal adhesion kinase, and cadherin indicate cooperative roles during zebrafish morphogenesis. *Mol. Biol. Cell* **14**, 3065-3081.
Crump, J. G., Swartz, M. E. and Kimmel, C. B. (2004). An integrin-dependent role of pouch endoderm in hyoid cartilage development. *PLoS Biol.* **2**, E244.
Cukierman, E., Pankov, R., Stevens, D. R. and Yamada, K. M. (2001). Taking cell-matrix adhesions to the third dimension. *Science* **294**, 1708-1712.
Davidson, L. A., Keller, R. and DeSimone, D. W. (2004). Assembly and remodeling of the fibrillar fibronectin extracellular matrix during gastrulation and neurulation in Xenopus laevis. *Dev. Dyn.* **231**, 888-895.
Davis, S., Gale, N. W., Aldrich, T. H., Maisonpierre, P. C., Lhotak, V., Pawson, T., Goldfarb, M. and Yancopoulos, G. D. (1994). Ligands for EPH-related receptor tyrosine kinases that require membrane attachment or clustering for activity. *Science* **266**, 816-819.
Davy, A. and Soriano, P. (2007). Ephrin-B2 forward signaling regulates somite patterning and neural crest cell development. *Dev. Biol.* **304**, 182-193.
Durbin, L., Brennan, C., Shiomi, K., Cooke, J., Barrios, A., Shanmugalingam, S., Guthrie, B., Lindberg, R. and Holder, N. (1998). Eph signaling is required for segmentation and differentiation of the somites. *Genes Dev.* **12**, 3096-3109.
Durbin, L., Sordino, P., Barrios, A., Gering, M., Thisse, C., Thisse, B., Brennan, C., Green, A., Wilson, S. and Holder, N. (2000). Anteriorposterior patterning is required within segments for somite boundary formation in developing zebrafish. *Development* **127**, 1703-1713.
Dzamba, B. J., Jakab, K. R., Marsden, M., Schwartz, M. A. and DeSimone, D. W. (2009). Cadherin adhesion, tissue tension, and noncanonical Wnt signaling regulate fibronectin matrix organization. *Dev. Cell* **16**, 421-432.
Galbraith, C. G., Yamada, K. M. and Galbraith, J. A. (2007). Polymerizing actin fibers position integrins primed to probe for adhesion sites. *Science* **315**, 992-995.
Georges-Labouesse, E. N., George, E. L., Rayburn, H. and Hynes, R. O. (1996). Mesodermal development in mouse embryos mutant for fibronectin. *Dev. Dyn.* **207**, 145-156.
Ginsberg, M. H., Partridge, A. and Shattil, S. J. (2005). Integrin regulation. *Curr. Opin. Cell Biol.* **17**, 509-516.
Goto, T., Davidson, L., Asashima, M. and Keller, R. (2005). Planar cell polarity genes regulate polarized extracellular matrix deposition during frog gastrulation. *Curr. Biol.* **15**, 787-793.
Holley, S. A. (2007). The genetics and embryology of zebrafish metamerism. *Dev. Dyn.* **236**, 1422-1449.
Holley, S. A., Geisler, R. and Nüsslein-Volhard, C. (2000). Control of *her1* expression during zebrafish somitogenesis by a *Delta*-dependent oscillator and an independent wave-front activity. *Genes Dev.* **14**, 1678-1690.
Hynes, R. O. (2002). Integrins: bidirectional, allosteric signaling machines. *Cell* **110**, 673-687.
Irie, A., Kamata, T., Puzon-McLaughlin, W. and Takada, Y. (1995). Critical amino acid residues for ligand binding are clustered in a predicted beta-turn of the third N-terminal repeat in the integrin alpha 4 and alpha 5 subunits. *EMBO J.* **14**, 5550-5556.
Jülich, D., Geisler, R., the Tübingen 2000 Screen Consortium and Holley, S. A. (2005). Integrinα5 and Delta/Notch signalling have complementary spatiotemporal requirements during zebrafish somitogenesis. *Dev. Cell* **8**, 575-586.
Kabat, E. A., Wu, T. T., Reid-Miller, M., Perry, H. M. and Gottesman, K. S. (1987). *Sequences of Proteins of Immunological Interest*. Washington, DC: United States Department of Health and Human Services.
Kerppola, T. K. (2008). Bimolecular fluorescence complementation (BiFC) analysis as a probe of protein interactions in living cells. *Annu. Rev. Biophys.* **37**, 465-487.
Koshida, S., Kishimoto, Y., Ustumi, H., Shimizu, T., Furutani-Seiki, M., Kondoh, H. and Takada, S. (2005). Integrinalpha5-dependent fibronectin accumulation for maintenance of somite boundaries in zebrafish embryos. *Dev. Cell* **8**, 587-598.
Kragtorp, K. A. and Miller, J. R. (2007). Integrin alpha5 is required for somite rotation and boundary formation in Xenopus. *Dev. Dyn.* **236**, 2713-2720.
Larsen, M., Artym, V. V., Green, J. A. and Yamada, K. M. (2006). The matrix reorganized: extracellular matrix remodeling and integrin signaling. *Curr. Opin. Cell Biol.* **18**, 463-471.
Mao, Y. and Schwarzbauer, J. E. (2005a). Fibronectin fibrillogenesis, a cell-mediated matrix assembly process. *Matrix Biol.* **24**, 389-399.
Mao, Y. and Schwarzbauer, J. E. (2005b). Stimulatory effects of a three-dimensional microenvironment on cell-mediated fibronectin fibrillogenesis. *J. Cell Sci.* **118**, 4427-4436.
Mould, A. P., Askari, J. A., Barton, S., Kline, A. D., McEwan, P. A., Craig, S. E. and Humphries, M. J. (2002). Integrin activation involves a conformational change in the alpha 1 helix of the beta subunit A-domain. *J. Biol. Chem.* **277**, 19800-19805.
Mould, A. P., Symonds, E. J., Buckley, P. A., Grossmann, J. G., McEwan, P. A., Barton, S. J., Askari, J. A., Craig, S. E., Bella, J. and Humphries, M. J. (2003). Structure of an integrin-ligand complex deduced from solution x-ray scattering and site-directed mutagenesis. *J. Biol. Chem.* **278**, 39993-39999.
Mould, A. P., Travis, M. A., Barton, S. J., Hamilton, J. A., Askari, J. A., Craig, S. E., Macdonald, P. R., Kammerer, R. A., Buckley, P. A. and Humphries, M. J. (2005). Evidence that monoclonal antibodies directed against the integrin beta subunit plexin/semaphorin/integrin domain stimulate function by inducing receptor extension. *J. Biol. Chem.* **280**, 4238-4246.
Mould, A. P., McLeish, J. A., Huxley-Jones, J., Goonesinghe, A. C., Hurlstone, A. F., Boot-Handford, R. P. and Humphries, M. J. (2006). Identification of multiple integrin beta1 homologs in zebrafish (Danio rerio). *BMC Cell Biol.* **7**, 24.
Nikaido, M., Kawakami, A., Sawada, A., Furutani-Seiki, M., Takeda, H. and Araki, K. (2002). Tbx24, encoding a T-box protein, is mutated in the zebrafish somite-segmentation mutant fused somites. *Nat. Genet.* **31**, 195-199.
Nüsslein-Volhard, C. and Dahm, R. (2002). *Zebrafish: A Practical Approach* (ed. B. D. Hames), pp. 303. Oxford: Oxford University Press.
Pankov, R., Cukierman, E., Katz, B. Z., Matsumoto, K., Lin, D. C., Lin, S., Hahn, C. and Yamada, K. M. (2000). Integrin dynamics and matrix assembly: tensin-dependent translocation of alpha(5)beta(1) integrins promotes early fibronectin fibrillogenesis. *J. Cell Biol.* **148**, 1075-1090.
Pasquale, E. B. (2008). Eph-ephrin bidirectional signaling in physiology and disease. *Cell* **133**, 38-52.
Saka, Y., Hagemann, A. I. and Smith, J. C. (2008). Visualizing protein interactions by bimolecular fluorescence complementation in Xenopus. *Methods* **45**, 192-195.
Shimaoka, M., Takagi, J. and Springer, T. A. (2002). Conformational regulation of integrin structure and function. *Annu. Rev. Biophys. Biomol. Struct.* **31**, 485-516.
Trinh, L. A. and Stainier, D. Y. (2004). Fibronectin regulates epithelial organization during myocardial migration in zebrafish. *Dev. Cell* **6**, 371-382.
Valdramidou, D., Humphries, M. J. and Mould, A. P. (2008). Distinct roles of beta1 metal ion-dependent adhesion site (MIDAS), adjacent to MIDAS (ADMIDAS), and ligand-associated metal-binding site (LIMBS) cation-binding sites in ligand recognition by integrin alpha2beta1. *J. Biol. Chem.* **283**, 32704-32714.
van Eeden, F. J. M., Granato, M., Schach, U., Brand, M., Furutani-Seiki, M., Haffter, P., Hammerschmidt, M., Heisenberg, C. P., Jiang, Y. J., Kane, D. A. et al. (1996). Mutations affecting somite formation and patterning in the zebrafish *Danio rerio*. *Development* **123**, 153-164.
Wierzbicka-Patynowski, I. and Schwarzbauer, J. E. (2003). The ins and outs of fibronectin matrix assembly. *J. Cell Sci.* **116**, 3269-3276.
Winklbauer, R. (1998). Conditions for fibronectin fibril formation in the early Xenopus embryo. *Dev. Dyn.* **212**, 335-345.
Xiong, J. P., Stehle, T., Zhang, R., Joachimiak, A., Frech, M., Goodman, S. L. and Arnaout, M. A. (2002). Crystal structure of the extracellular segment of integrin alpha Vbeta3 in complex with an Arg-Gly-Asp ligand. *Science* **296**, 151-155.
Xu, Q., Alldus, G., Holder, N. and Wilkinson, D. G. (1995). Expression of truncated Sek-1 receptor tyrosine kinase disrupts the segmental restriction of gene expression in the Xenopus and zebrafish hindbrain. *Development* **121**, 4005-4016.
Yang, J. T., Bader, B. L., Kreidberg, J. A., Ullman-Cullere, M., Trevithick, J. E. and Hynes, R. O. (1999). Overlapping and independent functions of fibronectin receptor integrins in early mesodermal development. *Dev. Biol.* **215**, 264-277.